Tang et al. Nanoscale Research Letters (2015) 10:276
DOI 10.1186/s11671-015-0977-1

Nanoscale Research Letters
a SpringerOpen Journal

NANO EXPRESS Open Access

Photocatalytic Property of TiO_2-Vermiculite Composite Nanofibers via Electrospinning

Chao Tang, Meiling Hu, Minghao Fang*, Yangai Liu, Xiaowen Wu, Wenjuan Liu, Meng Wang and Zhaohui Huang

Abstract

Titanium dioxide (TiO_2) is one of the most common photocatalysts. In this study, TiO_2-vermiculite composite nanofibers with a mesh structure and a diameter of approximately 300 nm were prepared via sol–gel approach combined with electrospinning technique. The samples were characterized by X-ray diffraction, scanning electron microscopy, ultraviolet–visible spectroscopy, etc. The photocatalytic property was also evaluated. The TiO_2-vermiculite composite nanofibers annealed at 550 °C for 3 h exhibited the best absorption and photo-degradation ability for the treatment of methylene blue. The results implied that the combination of mineral vermiculite powders with TiO_2 enhanced the absorption-degradation performance of the as-prepared photocatalytic materials, consequently promoting the materials' ability to degrade methylene blue.

Keywords: TiO_2; Vermiculite; Photocatalysis; Electrospinning

Background

Titanium dioxide (TiO_2) is one of the most common photocatalytic materials due to its unique energy band structure and non-toxicity. Several methods have been reported to synthesize TiO_2 nanoparticles, nanowires, nanotubes, nanofibers, etc. However, most of the photocatalytic materials currently used consist of nanoparticles [1]. But the photodegradation rate of photocatalytic materials is rather low because the powders easily agglomerate. Moreover, the band gap of TiO_2 is 3.2 eV, which is an intrinsic property of the material. Decreasing the energy band would allow for the activity of TiO_2 by UV light, which accounts for 5 % of the whole spectrum of sunlight. Therefore, broadening the responding spectral region of TiO_2 is an effective method to increase the photocatalytic property of such materials [2, 3].

Electrospinning is a novel way to obtain one-dimensional inorganic nanofibers, such as TiO_2, ZnO, Al_2O_3, SnO_2, and $BaTiO_3$. The electrospinning equipment consists of a high-voltage power supply, a spinneret, a syringe pump, and a collector. The precursor solution is jetted by the high-voltage power supply via the spinneret and the syringe pump, and nanofibers can then be obtained on the collector. By controlling the viscosity of the precursor, the high-voltage strength, and the distance between the spinneret and the collector, which could all affect the diameter and morphology of the nanofibers, we were able to obtain TiO_2 polymers and amorphous TiO_2 by annealing the nanofibers prepared via the electrospinning process [4, 5]. Vermiculite is a low cost and abundant layered silicate mineral raw material. It features a large surface area and specific absorption property. The nanofiber photocatalytic material used in this study was obtained by combing vermiculite and TiO_2 nanofibers, which increases the volume surface area of the composites fibers and promotes the fibers' ability to decompose chemical wastes materials [6, 7].

In this study, vermiculite and TiO_2 composite nanofibers were synthesized by combining the sol–gel process with the electrospinning technique. The photocatalytic ability of the nanofiber composites was assessed by studying the degradation of methylene blue (MB) under irradiation with UV light. The results showed that the utilization of TiO_2 composite nanofibers containing 2 wt.% of vermiculite resulted in a remarkable absorption and an enhanced degradation of MB.

Methods

Synthesis of the TiO_2-Vermiculite Composite Nanofibers

The initial step in the synthesis of the TiO_2-vermiculite composite nanofibers was the preparation of a precursor

* Correspondence: fmh@cugb.edu.cn
School of Materials Science and Technology, Beijing Key Laboratory of Materials Utilization of Nonmetallic Minerals and Solid Wastes, National Laboratory of Mineral Materials, China University of Geosciences (Beijing), Beijing 100083, China

© 2015 Tang et al. This is an Open Access article distributed under the terms of the Creative Commons Attribution License (http://creativecommons.org/licenses/by/4.0), which permits unrestricted use, distribution, and reproduction in any medium, provided the original work is properly credited.

via the sol–gel process. To fabricate the precursor, 1.5 g of polyvinyl pyrrolidone (PVP, Mc = 1,300,000, Alfa Aesar), 20 ml of ethanol, 5 ml of acetic acid, and 5 ml of tetrabutyltitanate were mixed with different amounts of vermiculite powders and stirred for 2 h to ensure a homogeneous mixture. The obtained precursors were then transferred into the electrospinning instrument to fabricate the vermiculite/PVP/$Ti(OCH(CH_3)_2)_4$ nanofibers. An electrical potential of 15 kV was applied between the nozzle and the collector in order to eject the sol–gel precursor to the collection board which was installed a distance of 15 cm to the nozzle. In order to obtain nanofibers with a homogenous size distribution, the propulsion speed was set to 2 ml/h. After a thermal treatment for 3 h at 550 °C, the vermiculite/PVP/$Ti(OCH(CH_3)_2)_4$ fibers were transformed into TiO_2-vermiculite composite nanofibers.

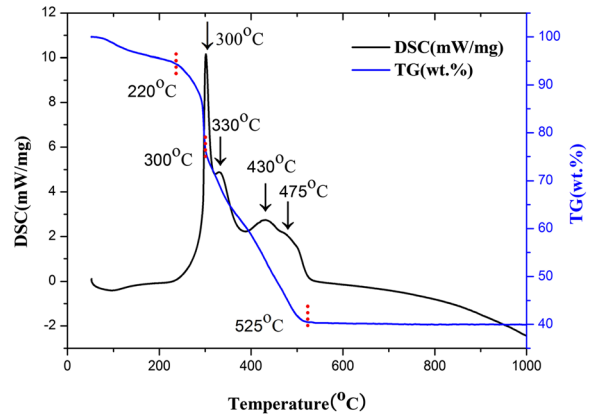

Fig. 1 TG-DSC curve obtained for the PVP/$Ti(OCH(CH_3)_2)_4$ composite nanofibers in air

Characterization

The vermiculite/PVP/$Ti(OCH(CH_3)_2)_4$ fibers were characterized by the simultaneous application of thermogravimetry and differential scanning calorimetry (TG-DSC). The phase composition of the TiO_2-vermiculite composite nanofibers was studied by D/max-rA X-ray diffraction (XRD, Rigaku Corporation, Japan, Cu Kα radiation, λ = 1.5406 Å). The microstructures and nanostructures of the nanofibers were characterized by scanning electron microscopy (SEM, JEOL JSM6700F, Japan) and transmission electron microscopy (TEM, 300 kV, FEI-tecnai-G^3-F20, Philips, Netherlands). The nanofibers were ultrasonically dispersed in ethanol and then dropped onto carbon-coated copper grids prior to the TEM investigations. Diffuse reflectance ultraviolet–visible (UV–vis) absorption spectra were recorded using a Carry 5000 UV–vis-NIR spectrophotometer with an integrating sphere attachment.

The photocatalytic property of the nanofibers was evaluated as follow: the nanofiber samples were suspended into the MB solution (10 mg/L) and the solution was stirred for 30 min under exclusion of light. The adsorption equilibrium of the solution was reached when the methylene blue concentration remained in balance. Then, the solution was stirred by magnetic stirring and irradiated with UV light using a 500 W high-pressure mercury lamp performance in order to evaluate the photocatalytic property. A 3 ml of the pollutant solution was sampled every 20 min and centrifuged for the separation of the upper clear solution. The concentration of MB was analyzed using a UV–vis spectrophotometer (L5, INESA) at the characteristic wavelength of 664 nm.

Results and Discussion

The results of TG-DSC analyses of the PVP/$Ti(OCH(CH_3)_2)_4$ composite nanofibers are shown in Fig. 1. The TG curves feature four distinct stages of weight loss: a weight loss of 5 % was observed when the temperature was increased from room temperature to 220 °C, a loss of 19 % occurred when the temperature was increased from 220 to 300 °C, another loss of 36 % occurred when the temperature was further increased from 300 to 525 °C, where no weight loss was detected for temperatures above 525 °C. The first weight loss was attributed to the evaporation of ethanol and water in the sample. The second weight loss, corresponding to the sharp peak in the DSC curve, was attributed to the decomposition of PVP side chain [8, 9]. Three exothermic peaks were observed during the third weight loss period in the temperature range from 300 to 430 °C, which were linked to the degradation of the PVP main chain and $Ti(OCH(CH_3)_2)_4$. The formation of the anatase phase of TiO_2 began at a temperature of 475 °C. The phase transformation from the anatase phase to the rutile phase was completed for temperatures above 525 °C [10, 11].

Figure 2 shows the XRD spectra obtained for the TiO_2-vermiculite composite nanofibers calcined at 550 °C for 3 h. The samples were mainly consist of anatase and rutile TiO_2. The Anatase and rutile TiO_2 are the main phases in pure TiO_2 with more rutile TiO_2 observed than anatase TiO_2. After calcination of the composite nanofibers at temperatures of up to 550 °C, the anatase phase was the major phase in the pure TiO_2, and only a small trace of the rutile phase remained. With the increase of the vermiculite mass fraction, the intensity of the peak of corresponding to the rulite phase increased compared to the corresponding peak observed for the pure TiO_2 nanofibers. Interestingly, the anatase phase was only detected when at least 2 wt.% of vermiculite or more was added to the TiO_2. Both the anatase and the rutile phase were found in the composite nanofibers after calcination, with the fraction of the anatase phase being higher than the fraction of the rutile phase. With the increase of the vermiculite mass fraction, the fraction of the rutile phase in the TiO_2-vermiculite composite nanofibers significantly

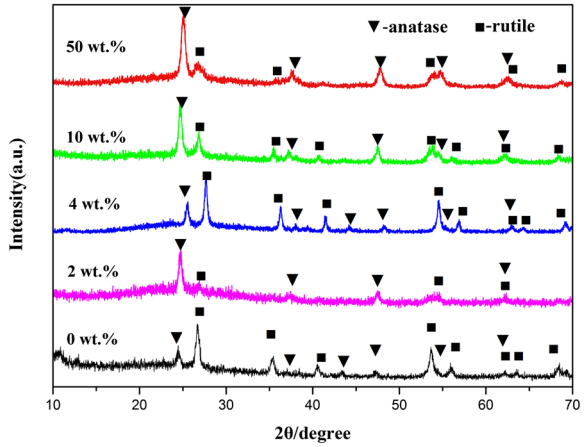

Fig. 2 XRD patterns obtained for TiO_2 nanofibers with a different vermiculite mass fraction(2 wt.%, 4 wt.% and 10 wt.%, 50 wt.%) and pure TiO_2 nanofibers prepared at 550 °C for 3 h

increased. Evidently, the addition of vermiculite had an effect on the phase composition of the TiO_2 nanofibers.

Figure 3a shows SEM micrographs of the TiO_2-vermiculite composite nanofibers with 2 wt.% vermiculite. It can be clearly seen that the samples contained smooth and continuous nanofibers with a diameter between 250 and 300 nm. In Fig. 3b, vermiculite particle was found among the TiO_2 nanofibers. Such particles can adsorb the pollutant and increase the concentration of the reactants thereby promoting the degradation reaction. However, when the number of vermiculite particles in the composites increases, the available amount of the TiO_2 catalyst decreases and the photocatalytic property is reduced.

Both the anatase and the rutile phase were found in the composite nanofibers exposed to the thermal treatment at 550 °C (Fig. 3c). In addition, the electron diffraction

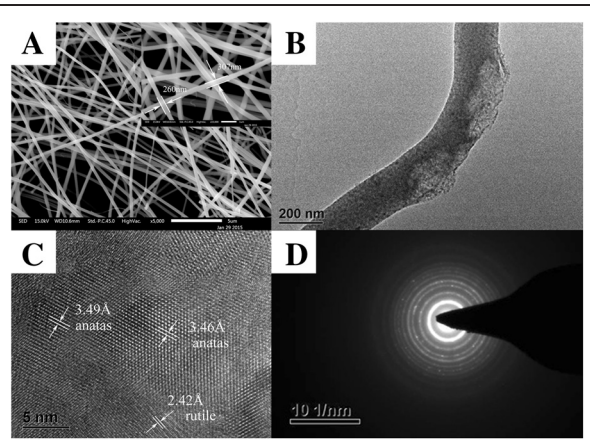

Fig. 3 a, **b** Microtopography of the TiO_2-vermiculite composite nanofibers with 2 wt.% vermiculite, **c** HRTEM micrograph of the TiO_2-vermiculite composite nanofibers with 2 wt.% vermiculite, **d** electron diffraction pattern obtained for the composite nanofibers

pattern obtained for the TiO_2-vermiculite composite nanofibers also revealed that the nanofibers are polycrystalline. As demonstrated in literature, the coexistence of the anatase and the rutile phase may enhance the photocatalytic property [12, 13]. Therefore, for a suitable TiO_2 nanofibers to vermiculite particle ratio (here, 2 wt.% of vermiculite particles), the TiO_2-vermiculite composite nanofibers show an optimized photocatalytic property.

Figure 4a shows the photocatalytic degradation behavior of TiO_2-vermiculite composite nanofibers for the degradation of MBin a solution with an MB concentration of 10 mg/L. As shown in Fig. 4a, the initial MB concentration is lower than 100 % after stirring for 30 min under exclusion of light. Furthermore, the MB concentration is lower when the amount of vermiculite in the nanofibers is higher. In this adsorption process, the vermiculite acts as an adsorbing material. Under irradiation with UV light, the composite nanofibers degrade the MB in the solution, which is a photodegradation process. Therefore, in the experiments, an adsorption-photodegradation process occurred. As a result, the samples containing 2 wt.% vermiculite showed the best adsorption and photocatalytic behavior. Compared with the pure TiO_2 nanofibers, for the TiO_2 composite nanofibers containing 2 wt.% vermiculite, the reaction equilibrium is reached earlier.

The photodegradation rate is an important factor for the evaluation of photocatalytic materials. Figure 4b compares the degradation rate of the samples. In Fig. 4b, the slope of the line corresponds to the reaction rate of the photodegradation process. The degradation rate of the TiO_2 nanofibers with 2 wt.% vermiculite nanoparticles is the highest among all samples. This can be explained as follows: The degradation process is caused by the TiO_2. With an increasing amount of vermiculite and a decreasing amount of the catalyst (TiO_2), the absorbability is enhanced, whereas the catalytic ability is reduced at the same time. Therefore, the TiO_2 nanofibers with 2 wt.% vermiculite nanoparticles show stronger capabilities (including adsorption and photocatalysis) to treat chemical pollutions.

The UV–vis absorption spectra of the TiO_2 composite nanofibers with different vermiculite mass fraction are compared in Fig. 5a, displaying the absorption spectra for each sample for an excitation wavelength of approximately 400 nm (3.10 eV). The band gap energy (E_g) for each sample was obtained by plugging the absorption data into the direct transition equation:

$$\alpha h\upsilon = E_D\left(h\upsilon - E_g\right)^{1/2}$$

α - optical absorption coefficient;
υ - photon energy;
E_g - direct band gap;
h *and* E_D - a constant.

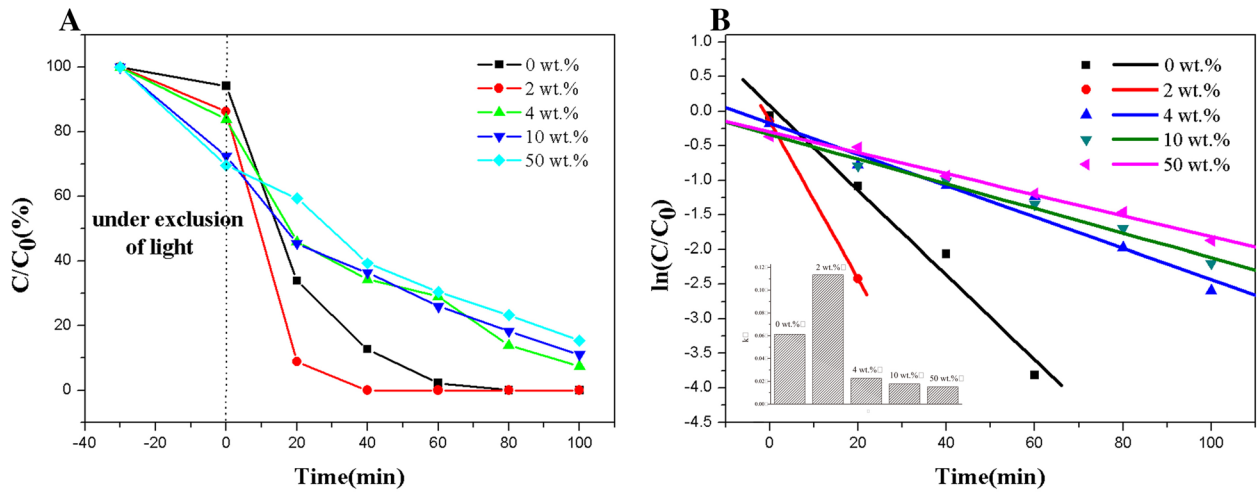

Fig. 4 Comparison of the photocatalytic degradation of methylene blue by TiO_2 nanofibers with different vermiculite mass fraction prepared at 550 °C for 3 h (**a** degradation curve, **b** kinetic curve)

The tangent to the curves (Fig. 5b) at the point of intersection with the x-axis corresponds to the direct band gap energy (E_g) of the samples, which are 3.05, 3.14, 3.08, 3.17, and 3.18 eV for a vermiculite mass fraction of 0, 2, 4, 10, and 50 wt.%, respectively [Additional files 1, 2, 3, 4 and 5]. The band gap energy increases with the amount of vermiculite in the nanofibers (Fig. 5b). The band gap energy of pure TiO_2 nanofibers is 3.05 eV due to the band alignment of the rutile and anatase TiO_2 phase. Moreover, the addition of a small amount of vermiculite to the TiO_2 nanofibers significantly changed the band gap energy. However, adding a larger amount of vermiculite to the nanofibers had negative effect on the band gap. In this paper, the composite nanofibers with 2 wt.% vermiculite showed the most suitable direct band gap and the highest photocatalytic activity.

Conclusions

TiO_2-vermiculite nanofiber composites were synthesized by combining a sol–gel process with the electrospinning technique. The TiO_2-vermiculite nanofiber composites were obtained after thermal treatment at 550 °C for 3 h. The results of the phase composition analysis indicate that the main phase of the prepared samples was the anatase phase, and a small amount of the rutile phase could also be detected. The analysis of the structure of the composite nanofibers revealed a smooth surface and diameter of approximately 300 nm. The photodegradation

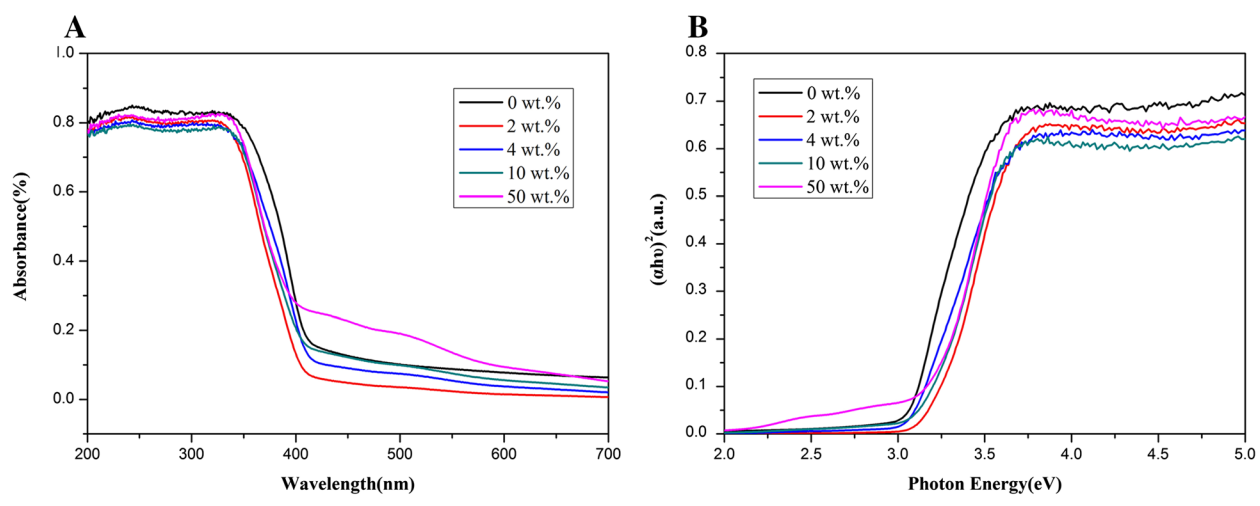

Fig. 5 a Comparison of the UV–vis absorption spectra obtained for TiO_2 nanofibers with different vermiculite mass fractions calcined in air at 550 °C for 3 h and **b** $(ahu)^2$ plotted as a function of the photon energy, E_g, for the different TiO_2-vermiculite composite nanofibers

of methylene blue by the as-prepared TiO_2-vermiculite composite nanofibers was performed under irradiation lights. In this study, the addition of the mineral powder to the TiO_2 nanofibers was demonstrated to enhance the adsorption-photocatalytic performance of the photocatalytic material.

Additional files

Additional file 1: *(ahu)*^{2} **plotted as a function of the photon energy,** ***Eg*****, for pure TiO_2 nanofibers.**

Additional file 2: *(ahu)*^{2} **plotted as a function of the photon energy,** ***Eg*****, for composite nanofibers with 2 wt.% vermiculite.**

Additional file 3: *(ahu)*^{2} **plotted as a function of the photon energy,** ***Eg*****, for composite nanofibers with 4 wt.% vermiculite.**

Additional file 4: *(ahu)*^{2} **plotted as a function of the photon energy,** ***Eg*****, for composite nanofibers with 10 wt.% vermiculite.**

Additional file 5: *(ahu)*^{2} **plotted as a function of the photon energy,** ***Eg*****, for composite nanofibers with 50 wt.% vermiculite.**

Competing interests
The authors declare that they have no competing interests.

Authors' contributions
CT, MH and MW independently completed this research. CT and MF participated in the design of the study and performed the statistical analysis and drafted the manuscript. CT participated in its design and revised this article. WL participated in a part of this experiment and the statistical analysis. ZH, YL and XW participated in revised this manuscript. All authors read and approved the final manuscript.

Acknowledgements
The authors greatly appreciate the Fundamental Research Funds for the Central Universities for financial support (grant nos. 2652015021 and 2652013051).

Received: 21 March 2015 Accepted: 12 June 2015
Published online: 01 July 2015

References
1. Woan K, Pyrgiotakis G, Sigmund W. Photocatalytic carbon-nanotube-TiO_2 composites. Adv Mater. 2009;21(21):2233–9.
2. Ni M, Leung MKH, Leung DYC, et al. A review and recent developments in photocatalytic water-splitting using TiO_2 for hydrogen production. Renew Sust Energ Rev. 2007;11(3):401–25.
3. Fujishima A, Zhang X, Tryk DA. TiO_2 photocatalysis and related surface phenomena. Surf Sci Rep. 2008;63(12):515–82.
4. Li D, Xia Y. Fabrication of titania nanofibers by electrospinning. Nano Lett. 2003;3(4):555–60.
5. Li H, Zhang W, Li B, et al. Diameter-dependent photocatalytic activity of electrospun TiO_2 nanofiber. J Am Ceram Soc. 2010;93(9):2503–6.
6. Chen Q, Wu P, Dang Z, et al. Iron pillared vermiculite as a heterogeneous photo-Fenton catalyst for photocatalytic degradation of azo dye reactive brilliant orange X-GN. Sep Purif Technol. 2010;71(3):315–23.
7. Wang L, Wang X, Cui S, et al. TiO_2 supported on silica nanolayers derived from vermiculite for efficient photocatalysis. Catal Today. 2013;216:95–103.
8. Daβler A, Feltz A, Jung J, et al. Characterization of rutile and anatase powders by thermal analysis. J Therm Anal. 1988;33(3):803–9.
9. Azhari SJ, Diab MA. Thermal degradation and stability of poly (4-vinylpyridine) homopolymer and copolymers of 4-vinylpyridine with methyl acrylate. Polym Degrad Stab. 1998;60(2):253–6.
10. Nuansing W, Ninmuang S, Jarernboon W, et al. Structural characterization and morphology of electrospun TiO_2 nanofibers. Mater Sci Eng B. 2006;131(1):147–55.
11. Li JY, Dai H, Li Q, et al. Lanthanum zirconate nanofibers with high sintering-resistance. Mater Sci Eng B. 2006;133(1):209–12.
12. Scanlon DO, Dunnill CW, Buckeridge J, et al. Band alignment of rutile and anatase TiO_2. Nat Mater. 2013;12(9):798–801.
13. Zhang J, Xu Q, Feng Z, et al. Importance of the relationship between surface phases and photocatalytic activity of TiO_2. Angew Chem Int Ed. 2008;47(9):1766–9.

Submit your manuscript to a SpringerOpen journal and benefit from:

- ► Convenient online submission
- ► Rigorous peer review
- ► Immediate publication on acceptance
- ► Open access: articles freely available online
- ► High visibility within the field
- ► Retaining the copyright to your article

Submit your next manuscript at ► springeropen.com